Staying on Track: a Comparative Study on the Use of Optical Flow in 360° Video to Mitigate VIMS

Paulo Bala
FCT, Universidade Nova de Lisboa & ITI-LARSys
Lisbon
paulo.bala@m-iti.org

Ian Oakley
Department of Human Factors Engineering, UNIST
Ulsan
secondauthor@email.com

Valentina Nisi
IST, Universidade de Lisboa & ITI-LARSys
Lisbon
valentina.nisi@m-iti.org

Nuno Nunes
IST, Universidade de Lisboa & ITI-LARSys
Lisbon
njn@m-iti.org

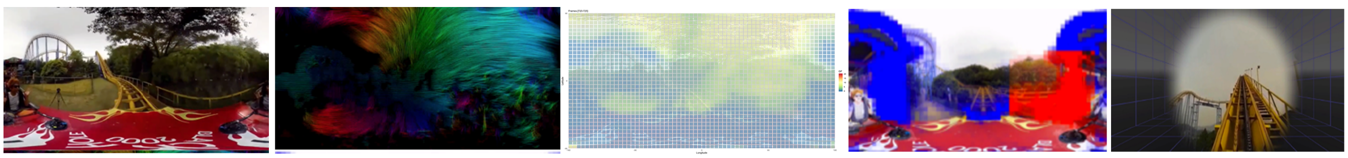

Figure 1: Optical flow sequence. From left to right: 360° video frame; precomputed optical flow using a Gunnar Farnebäck algorithm; representation of optical flow magnitudes; aggregation of optical flow values during runtime based on head direction; dynamic visual optimization based on the aggregated optic flow values.

ABSTRACT

Visually Induced Motion Sickness (VIMS), when the visual system detects motion that is not felt by the vestibular system, is a deterrent for first-time Virtual Reality (VR) users and can impact its adoption rate. Constricting the field-of-view (FoV) has been shown to reduce VIMS as it conceals optical flow in peripheral vision, which is more sensitive to motion. Additionally, several studies have suggested the inclusion of visual elements (e.g., grids) consistent with the real world as reference points. In this paper, we describe a novel technique dynamically controlled by a video's precomputed optical flow and participants' runtime head direction and evaluate it in a within-subjects study (N = 24) on a 360° video of a roller coaster. Furthermore, based on a detailed analysis of the video and participant's experience, we provide insights on the effectiveness of the techniques in VIMS reduction and discuss the role of optical flow in the design and evaluation of the study.

CCS CONCEPTS

• **Human-centered computing → Virtual reality**; *Usability testing*.

KEYWORDS

360° Video; Cinematic Virtual Reality; Optical Flow; Field of View Manipulation; Visually Induced Motion Sickness

ACM Reference Format:

Paulo Bala, Ian Oakley, Valentina Nisi, and Nuno Nunes. 2020. Staying on Track: a Comparative Study on the Use of Optical Flow in 360° Video to Mitigate VIMS. In *ACM International Conference on Interactive Media Experiences (IMX '20), June 17–19, 2020, Cornella, Barcelona, Spain.* ACM, New York, NY, USA, 12 pages. https://doi.org/10.1145/3391614.3393658

IMX '20, June 17–19, 2020, Cornella, Barcelona, Spain

ACM ISBN 978-1-4503-7976-2/20/06...$15.00
https://doi.org/10.1145/3391614.3393658

1 INTRODUCTION

Virtual Reality (VR) holds great promise as Head-Mounted Displays (HMDs) make their way out of the confines of research labs and into to the hands of consumers, bolstered by affordable VR hardware such as smartphones repurposed as HMDs. 360° video, one of the least technically demanding media in terms of production for this new wave of HMDs, is emerging as an expressive and engaging media for storytelling, journalism, and entertainment, among others [63]. However, several barriers (e.g., Human factors, such as comfort and safety of use) still need to be addressed to streamline the user's experience.

Visually induced motion sickness (VIMS), sometimes referred to as VR Sickness or Cybersickness, has symptoms similar to motion sickness [39], but occurs strictly from visual stimulation. VIMS has a multiple symptom profile (polysymptomatic) [57], including nausea, sweating, disorientation, among others. VIMS is also polygenic, meaning that symptoms manifest differently across individuals [57]. For example, women are more likely to manifest symptoms than men [4, 27, 28, 47, 51]. While there is extensive literature on prevention/reduction techniques, these techniques are mostly focused on computer-based VR (e.g., using runtime knowledge of the environment or player behavior [24]) and/or bespoke hardware solutions (e.g., curved surfaces for walking-based locomotion [48]). Focusing on 360° video, most of these techniques are not compatible (in terms of implementation/hardware) or are obtrusive to the user experience. Based on existing literature, we were motivated to understand how compatible VIMS reduction techniques [24, 53] could be applied to 360° video and its impact on the user experience. Furthermore, since we wanted to make these techniques less obtrusive to the user experience, we were motivated to understand how we could use 360° video itself as a control mechanism for the VIMS reduction techniques. Motivated by previous work [33], we explore how the 360° video's optical flow (a motion pattern caused by the relative motion of objects in the visual scene compared to the camera/observer) can contribute to these techniques and to contextualize their evaluation.

In this paper, we examine the role of optical flow, known to affect VIMS symptoms in VR, and how techniques known to reduce VIMS can be applied to 360° video. Connecting to the increasing need for design guidelines for VR and 360° video [6, 34, 43, 60], we ask two high-level research questions (RQs):

- RQ1 - *How can we use the optical flow of a 360° video to mitigate VIMS?*
- RQ2 - *How can we apply/combine techniques that mitigate VIMS in VR to 360° video?*

For the purpose of answering these RQs, we chose a popular 360° video [1], present in two datasets [42, 49], and calculated optical flow to be used at runtime (with an HMD) in controlling the parameters of techniques applied. We conducted a user study with two independent variables (both visual optimization techniques); both techniques are commonly used in VR and compatible with 360°. The first corresponds to an independent visual background (IVB) [53], where a virtual element (e.g., grid, horizon, nose) acts as a reference point of the real world inside the virtual world. The second corresponds to a restricted FoV (rFoV) [24, 33, 44, 50], where a virtual vignette (reduction of brightness towards the periphery of an image compared to the center) restricts the periphery of the user's vision, known to be more sensitive to optical flow. Table 1 presents the factorial combination of independent variables; for clearer writing, we refer to the terms baseline, IVB, rFoV & rFoV+IVB when describing and discussing results. For IVB, rFoV & rFoV+IVB, the optical flow is used to determine how much of the technique is visible to the user; a high optical flow (indicating movement) fully expresses the technique, while a low optical flow (stationary) "disables" the technique.

We contribute with a novel technique using the optical flow of 360° video to control parameters of techniques known to reduce Visually Induced Motion Sickness. We evaluate our proposed technique in a user study comparing and combining two techniques applicable to 360° video: independent visual background and restricted Field of View. Our findings suggest that restricted FoV aligned with optical flow, although intrusive in terms of Presence, is preferred and can promote exploration. Contextualizing participant behaviour with the media itself, we appraise the use of optical flow, identifying limitations and improvements for future work.

Table 1: Factorial Design with two independent variables. The color scheme of the combination cells are replicated across the paper

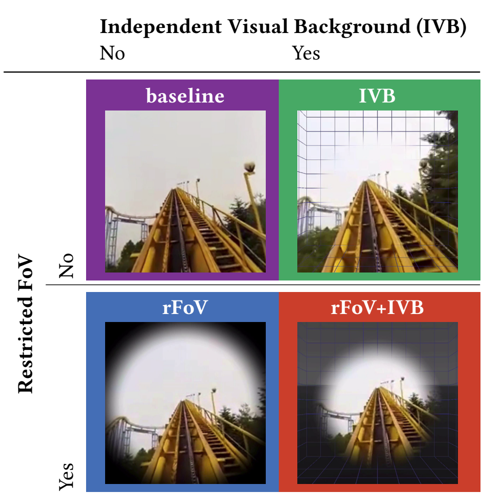

2 BACKGROUND AND RELATED WORKS

2.1 Visually Induced Motion Sickness (VIMS)

Simulator Sickness, resulting from exposure to VR systems, is most commonly assessed by the self-reported Simulator Sickness Questionnaire (SSQ) [35], categorizing symptoms into nausea (stomach awareness, sweating, salivation, among others), oculomotor (headaches, eye strain, among others) and disorientation (vertigo, dizziness, among others). The symptom profile that arises can be used to distinguish VIMS (whose main symptom is disorientation) from motion sickness (whose main symptom is nausea) from non-virtual simulator sickness (whose main symptom is oculomotor) [56]. Several theories have emerged to explain VIMS: the postural instability theory [58], that posits that the cause of VIMS is an inability to achieve proper balance after long periods of postural instability (such as a roller coaster); the Eye Movement Theory [22], that posits that the cause is tension in the muscle of the eyes that stimulate the vagus nerve; Rest Frame; Evolutionary [66]; among others [21, 57]. However, the most commonly supported is the Cue Conflict or Sensory Mismatch theory [57], that posits that symptoms arise when stimuli are being perceived differently by different senses; for example, in vection, there is a visual simulation that causes an illusion of motion, that is not compatible with the person's Vestibular system [39]. VIMS symptomatology and severity is variably diverse, being affected by age, gender, stress, anxiety and the physical qualities of the devices themselves [4, 14, 21, 36, 40].

2.2 VIMS Mitigation

For VIMS mitigation in model-based VR (virtual environment is entirely simulated by computer graphics renderings [63]), previous work puts emphasis on walking-based techniques [48] rather than on non-natural travel interfaces [8, 12]. High-precision low-latency tracking [24, 48] has been shown to reduce VIMS symptoms by matching physical movement in the real world to movement in the virtual environment but is limited to the size of the tracked environment. Tregillus' "walking-in-place" concept [65] uses smartphones' inertial sensors to simulate walking and offer proprioceptive feedback. Another walking-based technique Redirected Walking [55], dynamically and imperceptibly rotates the virtual environment, to keep users is a smaller physical area. However, walking-based techniques cannot be applied to 360° video, since they are not compatible with pre-recorded videos. 360° video compatible solutions focus on visual optimization (high frame rate rendering [24], latency reduction [2], brightness reduction [33], etc.). We provide an extended review of two VIMS mitigation techniques of particular relevance to this paper in the following subsections.

2.2.1 Field of View (FoV) Manipulation. Field of View manipulation has been known to mitigate VIMS symptoms successfully [4, 11, 24, 32, 36]. FoV can be characterized as display FoV (dFoV, area of the visual field occupied by the display; based on the physical system) and camera FoV (cFoV, area of the visual environment that is drawn in the display; based on the virtual system) [2]. Conceptually, dFoV should be the same as cFov to allow the virtual system to be overimposed correctly over the physical system; however, dFov is constrained by the technical capabilities of the hardware. Variations between them have been described as causing discomfort [17] (although, contrary evidence can also be found [46]). Previous works have shown that wide FoVs easily induce more symptoms compared to narrow FoVs [17]. The rationale behind this lies in the fact that users are more exposed to the visual periphery, an area more sensitive to motion [7, 13] causing vection. Newer HMDs try to increase their dFoV to match human vision [16, 72], increasing the sense of Presence [70].

On the opposite side, a broad range of work exists on restricting the FoV, reducing the access to the visual periphery. Wells and Venturino [67] used constant FoV to determine that smaller FoVs although reducing sickness, hamper tasks requiring a visual search. Kim et al. [38] used biosignal cybersickness detection systems to change FoV and discretely notify users to stop and relax; in this case, the system does not use FoV manipulation to prevent cybersickness, but rather to detect and correct, making it unsuitable for 360° video as it would interfere with the visualization of content and break the feeling of Presence. Fernandes and Feiner [24] used dynamic FoV restrictors (transparency circular hole with an inner and outer radius, acting as a vignette) based on gamepad input to reduce VIMS in model-based VR. Based on the previous work, McGill et al. [44] used peripheral blending of motion landscape and 360° video in the context of in-car VR to prevent symptoms caused by the car motion. Kala et al. [33] used dynamic vertical FoV to reduce VIMS when playing 360° video, basing FoV size on the visual analysis of the 360° video (feature extraction and Lucas-Kanade algorithm for optical flow). Their rationale behind merely reducing vertical FoV was to simulate blinking and to maintain adequate levels of Presence. While conceptually closest to our work, we differ in terms of terms of reproducibility (optical flow methods and parameters), implementation (VIMS reduction techniques) and stricter methodology (e.g., use of validated scales for sickness and Presence, among others). Finally, Nguyen et al. for their VR editing suite [50] use the content of the 360° video to control the FoV size when scrubbing through footage (vignettes contract faster in shaky scenes and slower in stable scenes).

2.2.2 Independent Visual Background. A common VIMS mitigation approach is the addition of visual elements such as an independent visual background such as grid as seen on Prothero et al.'s [53] work on IVBs on HMDs and Duh et al.'s [19, 20] work on IVB on a driving simulator. In these works, the IVB tethers the user to the real world as it remains stationary and locked to the user's position, regardless of the remainder of the virtual world. Lin et al. [41] expanded the design of IVB beyond the grid by testing natural IVB such as clouds; natural IVBs were perceived to be relatively stable and helped to reduce nausea. Additionally, Whittinghill et al. [68] proposed the use of virtual noses as anchors between the real and virtual world. To the best of our knowledge, there is no work on the application of IVB to 360° video, or its combination with other techniques.

3 USER STUDY

Based on the visual optimization techniques compatible with 360° video discussed above, and the potential to integrate video's optical flow as a control mechanism (RQ1), we chose to test the effectiveness and combination of restricted FoV and IVB in preventing VIMS symptoms (RQ2). The techniques chosen differ in their ability to mask the visual periphery that causes vection (e.g., a vignette covers more of the periphery than a grid) and their impact on Presence (as some techniques are more intrusive than others).

3.1 Experimental Design

The study uses a factorial design with two independent variables (IVB and restricted FoV, both with two levels - not present and present), resulting in 4 conditions (see Table 1). A repeated measures design was used to avoid grouping participants prone to motion sickness in one condition; to circumvent order effects, we used random allocation and scheduled only 4 sessions over a period of two weeks; to minimize after-exposure symptoms, sessions were separated by at least one day, participants were free to reschedule and the video stimulus used was shorter than most studies in VIMS.

3.2 Media

Considering the goal of the study, we required a short video with considerable motion. Although similar studies use videos with longer durations, shorter videos with visual obstructions like shakiness are known to trigger VIMS symptoms [18]. The video chosen, produced by Moovr, is a popular 360° video [1] (at time of writing, with more than 35 million views) of a roller coaster track at Seoul Grand Park, at 30 fps and duration of 3'27". The video is present in a dataset of saliency maps of 360° videos [49] (that analyzes 1'02" to 2'14") and in a dataset of saliency maps and motion maps [42] (that analyzes 0'20" to 1'20" and classifies the video as fast-paced). Using satellite images and the original video, timecodes were mapped to track contour (see fig. 2) and segmented according to track features (see table 2). Considering the different subsegments and optical flow values, during analysis, we only compare S2 and S3, since they are slower and faster-paced, respectively. S1 and S4 are out of the scope of the paper since they reflect mostly stationary scenarios.

Table 2: Roller coaster subsegments with track description (see fig. 2) and optical flow (see fig. 3)

Subsegments		Frames	Time	Track Description	Optical Flow's pattern and peaks
S1	A	1-690	0'00"	Stationary in the station and production logo	Pattern is caused by leaving the station and transition to production logo
S2	A	691-870	0'28"	Initial "launch track"	Peaks result from the transition of the production logo to video and optical "noise" generated by trees
	B	871-2240	0'36"	Long "lift hill" with a "test hill"	Pattern is caused by passing light poles
	C	2241-2700	1'33'	180° "bank turn" to gain momentum	Peak corresponds to a "tester hill" and acceleration
S3	A	2701-2990	1'52'	"Double-dip" to gain speed	Peaks are drops in the "double-dip"
	B	2991-3230	2'04"	Two "360° helixes"	Peaks correspond to the "helixes";
	C	3231-3500	2'14"	"Bank turn", followed by a hill ending in a "head chopper" (track underneath another track)	Peaks corresponds to the "headchopper" that causes optical noise overhead
	D	3501-4200	2'25"	Long portion of "lift hills"	Pattern corresponds to the various drops and trees lining the tracks towards the end
S4	A	4201-4691	2'55"	"Brake run" with steady movement to the station	Peak correspond to entering the station that causes optical noise overhead

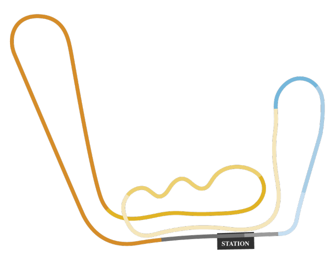

Figure 2: Top-down representation of the roller coaster track at Seoul Grand Park. Segments colors correspond to subsegments in table 2

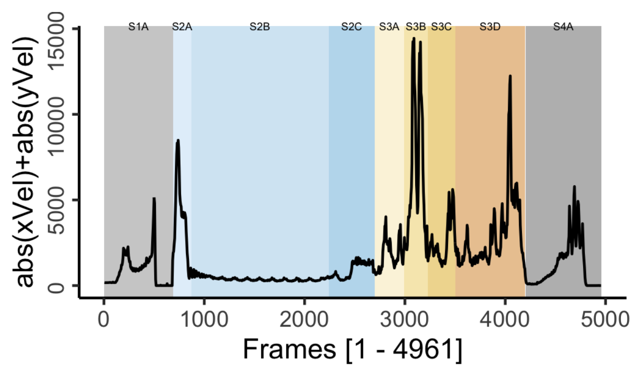

Figure 3: Optical Flow (sum of absolute optical flow vectors, abs(xVel) + abs(yVel)) across time (frames).

3.2.1 Optical Flow. Due to limitations in processing power of mobile HMDs, runtime computation of optical flow would affect rendering rates hindering the participant's experience; therefore we chose to precompute optical flow in XCode (release 9.2), using OpenFrameworks (release 0.9.8) with ofxOpenCV and ofxOpticalFlowFarneback [61]. Gunnar Farnebäck algorithm [23] is a dense optical flow algorithm calculating optical flow for all points in the video, unlike a sparse optical flow algorithm (like Lucas-Kanede[5]) that only calculates optical flow for some tracked points. The following settings were used: number of pyramid layers 2; image scale 0.3; number of search iterations per pyramid level 1; average filter/window size 10, with Gaussian filtering. Optical flow vectors (xVel and yVel) were saved to a comma-separated values (CSV) file; to reduce file size, readings were made every 5 frames, and pixel values were grouped in 5x5 pixel squares (resulting in a 72x36 grid). Fig. 1 illustrates the optical flow pipeline, while fig. 3 shows optical flow across time. Using fig. 3 as a basis, the peaks and patterns of optical flow are mapped to events or track features in table 2.

3.3 Implementation

The mobile VR application was made in Unity (release 2017.2), using Oculus Mobile SDK for Unity and "Tunneling Demo" [3] from Google Daydream Elements as a basis for the implementation of FoV restriction. During runtime, optical flow values based on head direction (corresponding to a square with 1/3 of video width as the side, centered on the user's head direction) were aggregated in a magnitude vector (sum of absolute values of optical flow's xVel and yVel) used to determine the size of the FoV. We empirically found that the relation between magnitude vector and FoV size worked better with a max magnitude of 60 corresponding to a min FoV of 30°, and a min magnitude of 10 corresponding to a max FoV of 60° (see table 3). At any moment, the FoV size was calculated from linear interpolation of these values and smooth damped (gradually changing a value towards a desired goal over time) over 0.3 seconds to prevent extreme flickering of FoV size. For example, if we input a constant optical flow from its minimum to its maximum (below 10 to above 50) and 0.3 second smooth dampening, the Fov would change from its min (30°) to its max (60°) at a maximum speed of 100°/s. During the viewing, head direction data (camera rotation quaternion) was recorded in XML files (Extensible Markup Files), later retrieved by the experimenter and converted into CSVs files in the Unity editor.

3.4 Experimental Setup

For this study, we used a Samsung Gear VR mobile HMD (SM-R322, 96° diagonal FOV) with a Samsung Galaxy S6 and V-Moda Crossfade M-100 over-ear headphones with XL cushions. All sessions

Table 3: Relation between Optical Flow magnitude and FoV for IVB, rFoV& rFoV+IVB

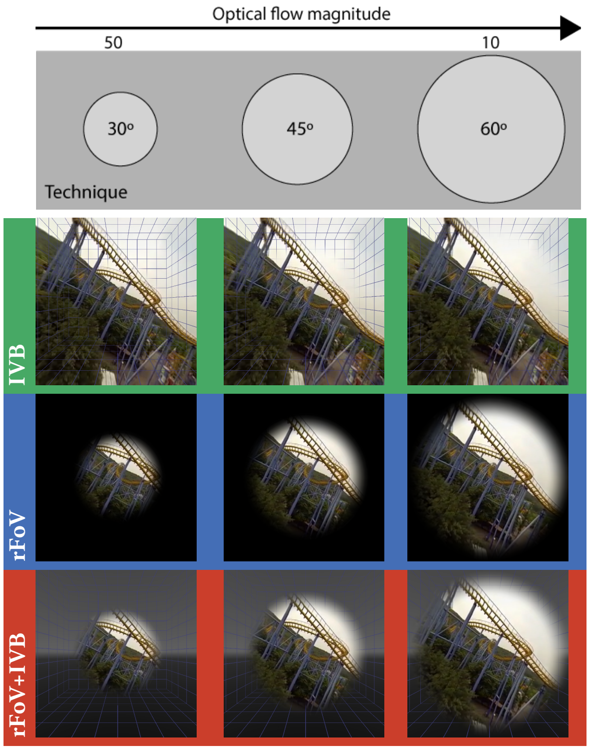

Table 4: Measures

Self-Reported	IPQ (Igroup Presence Questionnaire)
	ER (Experienced Realism)
	GP (General Presence)
	INV (Involvement)
	SP (Spatial Presence)
	SSQ (Simulator Sickness Questionnaire)
	D (Disorientation)
	N (Nausea)
	O (Oculo-Motor)
	TS (Total Score)
	PreTS (Absolute Total Score before exposure)
	PostTS (Absolute Total Score after exposure)
	VS (Visual Statement)
	VS1 ("I saw the virtual environment flicker")
	VS2 ("I saw visual elements that didn't belong to the virtual environment")
	VS3 ("I saw the virtual environment get brighter or dimmer")
	VS4 ("I saw the virtual environment change colors.")
	VS5 ("I felt like my field of view was changing in size.")
	MNVC (Most noticed visual change)
	SMNVC (Second most noticed visual change)
Objective	Axes (Yaw, Roll and Pitch)
	Geographic coordinates (Latitude and Longitude)
	S[1-4]-D (Accumulated distance for segment [1-4])
	S[1-4]-DP (Accumulated distance to POI for segment [1-4])

took place in meeting rooms in our research laboratory, clear of furniture that would obstruct the experience.

3.5 Measures

Participants were asked to fill out a Pre-Study Questionnaire with demographic information on gender, age, items (rating scale with seven levels "Never" to "Very often") on experience with VR, 360° VR and 360° video and the Motion Sickness Susceptibility Questionnaire Short-form (MSSQ-Short) [29].

Before each session, participants were asked to fill out a Pre-exposure SSQ [35]. After the session, they were again asked to fill out a Post-exposure SSQ; this resulted in relative (the difference between Post and Pre) and absolute (Post) values for 4 components (TS - TotalScore; N - Nausea; O - OculoMotor; D - Disorientation). After each session, participants also filled out the Igroup Presence Questionnaire (IPQ) [62], a validated Presence scale with 4 items (SP - Spatial Presence; INV - Involvement; ER - Experienced Realism; GP - General Presence).

Additional background variables were collected in the form of the three-section Visual Questionnaire (VQ), adapted from Fernandes et al. [24], to determine how noticeable the visual optimizations were, and how they affect Comfort, Enjoyability, and Desire. In the first section, Visual Statements (VS), participants are shown 5 Likert items (seven levels from "Did not notice or did not happen" to "Very obvious") with statements about possible visual changes that might have happened (VS1 to VS5). In the second section, Most Noticed Visual Change (MNVC), participants were asked if they saw any of the statements, identify it, and answer 4 Likert (seven levels) items: confidence ("Not confident" to "Very confident"), Comfort ("Not comfortable" to "Very comfortable"), Enjoyability ("Less enjoyable" to "More enjoyable") and Desire to have it in future VR experiences ("Don't want" to "Definitely want"). In the last section, MNVC questions were repeated as Second Most Noticed Visual Change (SMNVC). Participants were also allowed to leave any comment on the session in an open field.

Finally, head direction (quaternions) during the experience were converted into: Distance (D, angle between one recording to the next, in radians), Axes (Yaw, Pitch, Roll, in radians), geographic coordinates (Longitude and Latitude, in degrees), and Distance to POI (DP, the distance between head direction and location of POI, in radians). In this study, the POI is the roller coaster track, consistent with saliency maps of the video [49]. Table 4 summarizes the self-reported and objective measures used.

3.6 Experimental Procedure

Convenience sampling was used due to multiple constraints of the experiment (multiple sessions over two week period) that required participants to be readily available. Participants were recruited in-situ and through the institute's mailing list, and were not monetarily compensated for taking part in the study. In the first session, participants were handed an informed consent (detailing the goal of the study, but no information about conditions) form and Pre-Study Questionnaire. Before viewing any content, participants were asked to fill out a Pre-Session Questionnaire and then asked to assume a Romberg stance (standing up for the full experience, so that any changes in head movement data reflect postural sway), being given the HMD and headphones. Before viewing the content, participants could adjust the Gear's focus adjustment wheel and the experimenter would choose the correct condition using the Gear VR controller. After viewing, participants were asked to fill out a Post-Session questionnaire.

3.7 Sample

For this study, we did not assume any inclusion or exclusion criteria for the population, since VIMS susceptibility is influenced by several factors (like age, gender, health, previous experience with VR, among others). All participants (N = 24, 54% female) completed all four sessions. The mean age among participants was 29.4 years (SD = 5.8 years; range = 20-47). Beyond analysis with the **full population**, we repeated all analyses considering two other subpopulations. In the first, we only considered the **upper 75th percentile subpopulation** (from the MSSQ-short, meaning more prone to motion sickness) as done by the inclusion criteria of McGill et al[44], leaving us with a population of N = 13, 61% female. In the second, we only considered the **female subpopulation** (N = 13) since females are more susceptible to VIMS [4, 27, 28, 47, 51]. Additional subpopulations were not considered due to the small sample size. Unless explicitly stated, all statistical data reported, tables, and images correspond to the full population.

3.8 Analysis

Analysis was conducted in R [54], using a 2-tailed testing at α of .05 and figures were produced using the ggplot2 package [69]. Testing for Assumption of Normality was done through visual analysis of histograms/boxplots/Q-Q plots, analysis of Kurtosis and Skewness (and their standard errors), and normality tests (Shapiro-Wilk given that N<50). All data was shown to be nonparametric with the exception of SP and ER.

For parametric data, a factorial repeated measures ANOVA was performed using ezANOVA(), as prescribed by [26] and Holm-Bonferroni Method. For non-parametric data, we used a nonparametric equivalent [25] to the factorial repeated measures ANOVA, the Aligned Rank Transform (ART) [71]. For plots involving map projections, the following packages were used: sf [52], rgdal [10], spdep [9], and mapproj [45]. For hotspot analysis, we used a Getis-Ord Gi* algorithm, using 2-tailed testing at α of .05, consistent with Rothe and Hußmann [59] and Bala et al. [6].

Regarding the reporting and discussion of results in the following sections, for a clearer reading flow, we subdivided them according to the origin of the data as being from self-reported measures (sections 4 and 5) or from participant behaviour (sections 6 and 7).

4 RESULTS OF SELF-REPORTED MEASURES

4.1 Sample

In terms of motion sickness susceptibility, our population is representative of the general population since the mean raw score (MSSQRawScore) was 9.5 (SD = 10; range = 0-42), while the population norm is 12.90 (SD = 9.90) [29]. In terms of items related to previous experience with VR, most participants reported never (25%) or very seldom (25%) experiencing it (mdn = 1.5, iqr = 2.25). This inexperience is reinforced with the experience items for 360° VR (mdn = 1, iqr = 2) and 360° video (mdn = 1, iqr = 2), where most participants (42% in both cases) reported very seldom experience.

Table 5: Mean scores and standard deviations for IPQ and SSQ components across conditions, considering the full population

	baseline	IVB	rFoV	rFoV+IVB
GP	3.54±1.61	3.42±1.32	2.79±1.41	2.5±1.44
INV	3.2±.73	3.0±.82	3.04±.65	2.94±.76
ER	2.53±.66	2.5±.71	2.49±.53	2.39±.57
SP	3.43±1.26	3.33±1.28	3.17±1.11	2.55±1.8
TS	111.8±159	104.77±175	20.64±93.8	144.06±303
D	16.82±23	15.08±29	2.90±14.2	22.04±44
O	4.74±11	3.79±10	.63±7.4	8.53±25
N	8.35±14	9.14±18	1.99±8.4	7.95±16

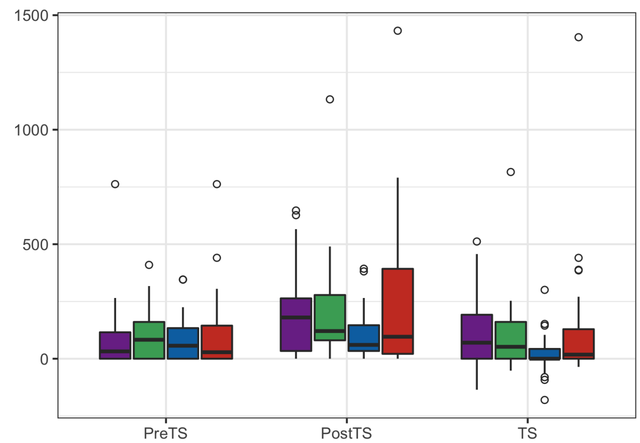

Figure 4: Boxplots with absolute (PreTS and PostTS) and relative (TS) for the SSQ component across conditions, considering the full population

4.2 IPQ & SSQ

Table 5 showcases the mean and standard deviation for IPQ and SSQ components: IPQ components are similar across techniques diverging for the GP and SP components; participants experiencing rFoV reported lower values for SSQ components. Fig. 4 shows the difference between absolute and relative TS values; a low relative TS median and compact distribution, as seen for rFoV, indicates that participants did not report symptoms, while a higher relative TS median and loose distributions, as seen for baseline, indicates that participants experienced VIMS. Considering the **full population**:

- a significant **main effect** on the use of **rFoV on SP** was found, F(1,23) = 6.4, η^2_G = .046, p<.05, indicating that SP scores in the absence of restricted FoV (see baseline, IVB in table 5) were significantly higher than in the presence of restricted FoV (see rFoV, rFoV+IVB in table 5).

- a significant **main effect** on the use of **rFoV on GP** was also found, F(1,69) = 9.34, p<.01, indicating that the GP scores in the absence of restricted FoV (see baseline, IVB in table 5) were significantly higher than in the presence of restricted FoV (see rFoV, rFoV+IVB in table 5).

Considering the subpopulation with only the **upper 75th percentile**:

- a significant **main effect** on the use of **rFoV on SP** was found, F(1,12) = 7.8, η_G^2 = .031, p<.05, indicating that SP scores in the absence of restricted FoV (baseline: 3.15 ± .89; IVB: 3.40 ± .73) were significantly higher than in the presence of restricted FoV (rFoV: 3.25 ± .85; rFoV+IVB: 2.71 ± 1.00).

Considering only the **female subpopulation**:

- a significant **main effect** on the use of **rFoV on SP** was found, F(1,12) = 8.6, η_G^2 = .042, p<.05, indicating that the SP scores in the absence of restricted FoV (baseline: 3.66 ± .95; IVB: 3.46 ± 1.11) were significantly higher than in the presence of restricted FoV (rFoV: 3.58 ± .98; rFoV+IVB: 2.66 ± 1.30).
- a significant **main effect** on the use of **IVB on INV** was found, F(1,36) = 5.66, p<.05, indicating that the INV scores in the absence of IVB (baseline: 3.27 ± .7; rFoV: 3.23 ± .62) were significantly higher than in the presence of IVB (IVB: 3.00 ± .72; rFoV+IVB: 2.77 ± .74).

4.3 Visual Questionnaire

4.3.1 Visual Statements. For visual statements, we look first at the statements that actually happened (VS2 and VS5), and summarize the remaining.

- **VS2** "I saw visual elements that didn't belong to the virtual environment": For baseline and rFoV, most participants (15 and 12, respectively) "did not notice"(baseline: mdn = 0, iqr = 2.25; rFoV: mdn = .5, iqr = 5). On the opposite side, for IVB and rFoV+IVB, most participants (13 and 9, respectively) reported VS2 as "very obvious" (IVB: mdn = 6, iqr = 2; rFoV+IVB: mdn = 5, iqr = 4.25).
- **VS5** "I felt like my field of view was changing in size": For baseline and IVB, most participants (19 and 12, respectively) "did not notice" (baseline: mdn = 0, iqr = .25; IVB: mdn = .5, iqr = 2). On the opposite side, for rFoV and rFoV+IVB, most participants (19 and 17, respectively) reported VS5 as "very obvious" (rFoV: mdn = 6, iqr = 0; rFoV+IVB: mdn = 6, iqr = 1.25).
- **VS1, VS3 & VS4**: Most participants did not notice VS1 (baseline: 9, mdn = 1, iqr = 3; rFoV: 9, mdn = 2, iqr = 4; rFoV+IVB: 6, mdn = 2, iqr = 3.5), altough for IVB, most participants reported 1 (7, mdn = 1, iqr = 3.5). Additionally, most participants did not notice VS3 (baseline: 13, mdn = 0, iqr = 2; IVB: 14, mdn = 0, iqr = 1.25; rFoV: 6, mdn = 2, iqr = 3.25; rFoV+IVB: 9, mdn = 2, iqr = 5) or VS4 (baseline: 15, mdn = 0, iqr = 1.25; IVB: 15, mdn = 0, iqr = 1.25; rFoV: 18, mdn = 0, iqr = .25; rFoV+IVB: 12, mdn = 0, iqr = 1).

4.3.2 Most and Second Most Noticed Visual Change. For MNVC, we look only at the visual changes that actually happened (VS2 and VS5) and the sessions where they happened (IVB, rFoV, and rFoV+IVB):

- For **IVB**, most participants (19, out of 23) correctly identified VS2 as the most noticeable, with a high degree of confidence (mdn = 6, iqr = 0); for these participants, most reported both comfort (mdn = 3; iqr = 1) and enjoyability (mdn = 3, iqr = 1.5), around the center of the scale. As for desire (mdn = 2, iqr = 3.5) most participants (8) reported disfavouring it.
- For **rFoV**, most participants (22, out of 24) correctly identified VS5 as the most noticeable visual change, with a high degree of confidence (mdn = 6, iqr = 0); values for comfort (mdn = 2.5, iqr = 3.25), enjoyability (mdn = 3, iqr = 2.5), and desire (mdn = 3, iqr = 2) were dispersed through the scale.
- For **rFoV+IVB**, most participants (14, out of 23) confidently (mdn = 6, iqr = 0) reported VS5 as the most noticeable visual change, followed by VS2 with 7 participants (mdn = 6, iqr = 1). For those that reported VS5, values were dispersed on the scale for confort (mdn = 2.5, iqr = 4), enjoyability (mdn = 3, iqr = 3) and desire (mdn = 3, iqr = 5). For those that reported VS2, values for confort (mdn = 2.5, iqr = 4), enjoyability (mdn = 1, iqr = 3) and desire (mdn = 0, iqr = 1) were concentrated on the lower end of the scale.

For SMNVC, we only looked at the visual changes that actually happened (VS2 and VS5) on **rFoV+IVB**; only 4 and 3 participants reported VS5 and VS2, respectively, with different confidence (VS5: mdn = 6, iqr = 0; VS2: mdn = 4). Values for confort, enjoyability, and desire, were all equal (VS5: mdn = 2.5, iqr = 3; VS2: mdn =2).

4.3.3 Feedback. At the end of each session, participants were given the choice to leave any feedback about difficulties they encountered. Participants are identified by P and their ID number. We report here only some relevant comments: about **baseline**, P6 "Removing the background music would make the experience more real"; about **IVB**, P4 "The grid was too distracting for me"; P10 "be more careful with the blue lines around visual field", P11 "grids from GearVR stood out from the video. The grids were high-res while the video was somewhat low-res"; about **rFoV**, P10 "Changing the view size makes me really uncomfortable, dizzy and if I stay more time I will be nauseated", P14 "I like having the field of view focused but sometimes the speed/size in which it changed was too fast, and that was a bit annoying"; about **rFoV+IVB**, P21 ox completely removed immersion in the virtual world", P12 "Some of the parts where the FoV got smaller were really strange to experience - my brain kept wanting to focus on the yellow track".

5 DISCUSSION OF SELF-REPORTED MEASURES

In McGill et al.'s study on Sickness for In-Car VR [44], they highlighted the difficulties in finding a suitable universal solution when the population is so diverse and that diversity factors into how these solutions are evaluated. Ideally, a solution for VIMS needs to be universal, to have a broad reach; on the other hand, it should not hinder the experience, leading to breaks in the feeling of Presence. The interplay between efficacy and invisibility is a critical point in the design of techniques to mitigate VIMS. Our design rationale by combining optical flow with established working techniques (known to reduce VIMS) tries to address this by having techniques that are effective, but that is only visible when needed.

In addition to difficulties in designing techniques for VIMS, studies on VIMS also encompass various methodological concerns (sampling, procedure, consistency of measures, among others) that restrain, complexify and/or diversify the design of evaluation studies. These methodological concerns impacted our study design in various ways. As examples: (1) although some studies on VIMS have used independent groups [37], we chose a repeated measures design due to polygenic symptom profiles of participants and to avoid grouping of susceptible participants in a technique, even though repeated measures can lead to habituation [30], (2) some studies [24, 44] compare only at post-exposure absolute SSQ scores, while we chose to compare absolute and relative scores (see fig. 4) to account for participants's profile. Overall, our sample is representative of the population in terms of susceptibility (based on the MSSQ values) and experience (based on experience items on VR). Since low susceptibility can hide results, some studies have opted [24, 44] to exclude participants; we opted to report the full population, as well as susceptible subpopulations, to better represent the effect of the techniques.

Overall, in terms of VIMS, the results presented are expected considering the short duration of the stimulus and the diverse population. By this, we mean that SSQ profiles D > N > O (across conditions) are consistent with the symptom profile for VIMS and that the effect of techniques like rFoV on VIMS reduction/mitigation is positive and promising, as seen in fig. 4. These SSQ profiles and effect for rFoV is also consistent for the subpopulations. Although short exposure times with considerable motion are sufficient to trigger VIMS symptoms [18], the video chosen may have been too short to cause stronger symptoms, since S3, the faster-paced segment, is less than a minute. As observable from table 5, the combination of IVB and restricted FoV is not beneficial since it reduces Presence and does not help reduce VIMS. Furthermore, using only IVB has limited effect on mitigating VIMS, since it may expose too much of the video. Additionally, comments made by the participants on the design of IVB (P4 "distracting"; P10 thinking that the grids were a mistake; P11 identifying the aesthetic quality of the grid as different from the video) detract from their usage and support Lin et al.'s [41] work on natural IVB.

In terms of Presence, the results presented are expected since the inclusion of techniques leads to lower levels of Presence by introducing noticeable visual interferences. From the Visual Statements, most participants correctly identified VS2 and VS5 in the sessions where they happened and confidently reported them in the MNVC and SMNV, therefore they were aware of the techniques. Participants for baseline reported higher Presence scores than for the remainder techniques (see table 5). Furthermore, this is confirmed by significant main effects on restricted FoV for the SP item for the full population and subpopulations and a significant main effect on restricted FoV for GP item in the full population. While we cannot differentiate baseline and IVB groups, these main effects suggest that since these conditions show more of the environment, they naturally result in higher Presence scores. Additionally, a significant main effect on IVB for INV item in the female subpopulation was also found; this might indicate that the presence of the grid is detrimental to the experience in terms of involvement, by introducing an element that breaks the immersion in the virtual environment, being consistent with the comments made by P4, P10, and P11 about IVB. As observable from table 5, the combination of IVB and restricted FoV is again not beneficial since it presented the lowest values for IPQ components. P14's comment "I like having the field of view focused but sometimes the speed/size in which it changed was to fast, and that was a bit annoying" can also indicate further refinements to restrictive FoV technique common in rFoV and rFoV+IVB. These could involve how the visual optimization techniques work in these conditions (e.g., the optical flow algorithm, the transition time of the adaptive restrictive FoV) or in different parameters (e.g., opacity of overlays).

Table 6: Mean scores and standard deviations for distance and distance to POI for S2 and S3, considering the full population

	baseline	IVB	rFoV	rFoV+IVB
S2-D	31.08±10	30.33±13	30.54±12	27.77±13
S2-DP	353.5±151	329.5±173	384±148	357.9±171
S3-D	14.3±6.1	16.7±12	15.9±7.7	14.3±7.3
S3-DP	126.9±43.7	148.0±76	144.1±60.7	138.2±69.8

6 RESULTS OF OBJECTIVE MEASURES

To contextualize the results of the self-reported measures and the impact of techniques on user experience, we analyzed the observed measures resulting from the participant behaviour. For each session, around 3970 camera rotation quaternions were recorded. Head movement was mapped to a time series for S2 and S3, see fig. 5, where the x-axis represents frames interval for S2 and S3. For fig. 5, several variables are mapped to the y-axis, namely yaw (side to side movement), roll (tilt), pitch (look up/down) and distance to POI (in this study, POI is the yellow track, consistent with saliency maps from [42, 49]). All values on the y-axis are in radians. From a visual analysis of fig. 5, there is more variation in yaw values than roll and pitch, since looking from side-to-side is more common in 360° video experiences. Furthermore, there is a clear difference between behaviour in S2 and S3: S2 across conditions show more variation in values until S2C (when the roller coaster starts to gain speed), in which case, the different conditions merge into similar behaviour. Furthermore, coupled with time series plots for Distance to POI (DP), a possible explanation emerges: during S2, participants are exploring the video (higher values of distance to POI means that they are distant from the track), but when S2C starts, participants focus their attention on the track direction.

Fig. 6 plots the accumulated distance (D, angle, in radians, between recordings) for S2 and S3. This accumulated distance can be conceived as a measurement of how much they move during an interval. While we cannot compare S2 and S3 since they have different time windows, we can compare conditions in each. From visual observation, regardless of conditions, D seems to be similar.

Table 6 represents the mean scores and standard deviations for distance (D) and distance to POI (DP) considering S2 and S3. D and DP showed to be non-parametric for both S2 and S3 in all subpopulations. Considering only a **female subpopulation**:

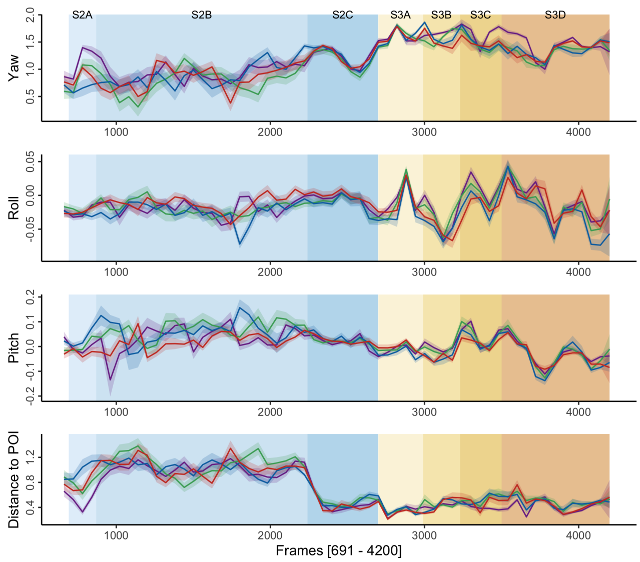

Figure 5: Time series for S2 and S3, considering the full population: x-axis is representative of frames; y-axis, from top to bottom: yaw, roll, pitch, distance to POI (DP)

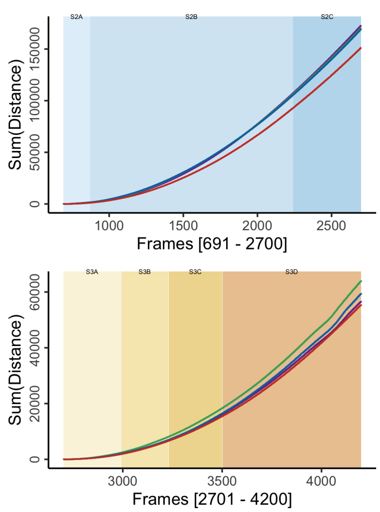

Figure 6: Time series for accumulated distances, considering the full population. From top to bottom: S2, S3

- For **S2**, a significant **main effect** on the use of **IVB on S2-D** was found, F(1,36) = 5.86, p<.05, indicating that the scores in the absence of IVB (baseline: 29.4 ± 10.22; rFoV: 28.9 ± 11.5) were significantly higher than in the presence of IVB (IVB: 26.74 ± 9.3; rFoV+IVB: 22.4 ± 11.1)
- For **S3**, a significant **main effect** on the use of **IVB on S3-D** was found, F(1,36) = 14.2, p<.001, indicating that scores in the absence of IVB (baseline: 13.38 ± 6.20; rFoV: 14.0 ± 7.1) were significantly higher than in the presence of IVB (IVB: 11.18 ± 6.25; rFoV+IVB: 9.92 ± 4.38)
- For **S3**, a significant **main effect** on the use of **IVB on S3-DP** was also found, F(1,36) = 13.99, p<.001, indicating that the scores in the absence of IVB (baseline: 121.9 ± 47.07; rFoV: 153.05 ± 78.17) were significantly higher than in the presence of IVB (IVB: 106.86 ± 38.22; rFoV+IVB: 109.31 ± 36.41)

For **S3** and using only the **upper 75th percentile subpopulation**, a main **interaction effect** on the use of **IVB and rFoV on S3-D** was found, F(1,36) = 4.14, p<.05. This was confirmed with post hoc analysis (p = .04, with Holm adjustment), meaning that adding IVB to restricted FoV (rFoV+IVB: 14.95 ± 8.22) resulted in less movement (baseline: 14.09 ± 7.19; IVB: 17.73 ± 15.07; rFoV: 18.48 ± 8.61).

Finally, fig. 7 represents a time series of hotspot maps (longitude and latitude of head direction) aggregated by S2 and S3 subsegments (see supplementary material for video of hotspots aggregated by smaller frame windows). Values of Getis-Ord Gi* are using a confidence interval of 95%. From a visual observation of fig. 7, S2 presents larger and disperse clusters of hotspots, representative of user's exploratory behaviour; S3, on the other hand, presents tighter clusters, centered around the track ahead (consistent with DP in Fig. 5). It is also worth noting that clusters are similar across conditions, implying that the techniques did not orient away from the POI.

7 GENERAL DISCUSSION

7.1 RQ1 - How can we use the optical flow of a 360° video to mitigate VIMS?

As evidenced by fig. 3, optical flow has potential to contextualize a video (e.g., the lamp posts in S2B) and to identify moments with potential extreme motion (e.g., the "helix" in S3B). Conceptually and in practice, its application to restrict FoV during areas of extreme motion and to widen it during stationary phase is successful. However, this potential is somewhat constrained by user behaviour. Analyzing the optical flow of video produced (see supplementary material), large areas of "noise" are usually located to the sides of the roller coaster train (e.g., trees in S3-D), while optical flow if you focus on the track is "medium". From fig. 5, fig. 7 and from the supplementary material, it is clear that when there are high values of optical noise (S3), participants were focused on the track (POI). This behaviour has multiple possible explanations: participants have prior experience and know the behaviour to adopt; participants know the direction they are headed; or as P10 stated: "my brain kept wanting to focus on the yellow track". Regardless of the reason, the type of media used and the participant's understanding of it affected the use of optical flow as a control mechanism for the techniques. We posit that the techniques might have been more effective if the video used did not have a defined POI. Furthermore, we also recognize that the noise produced by optical flow might be detrimental to the techniques used. For example, varying noise from optical flow can make the FoV contract and expand at a rate that participants find distracting or uncomfortable, as stated by P10 "Changing the view size makes me really uncomfortable, dizzy and if I stay more time I will be nauseated" and P14 "I like having the field of view focused but sometimes the speed/size in which it changed was too fast, and that was a bit annoying". We tried

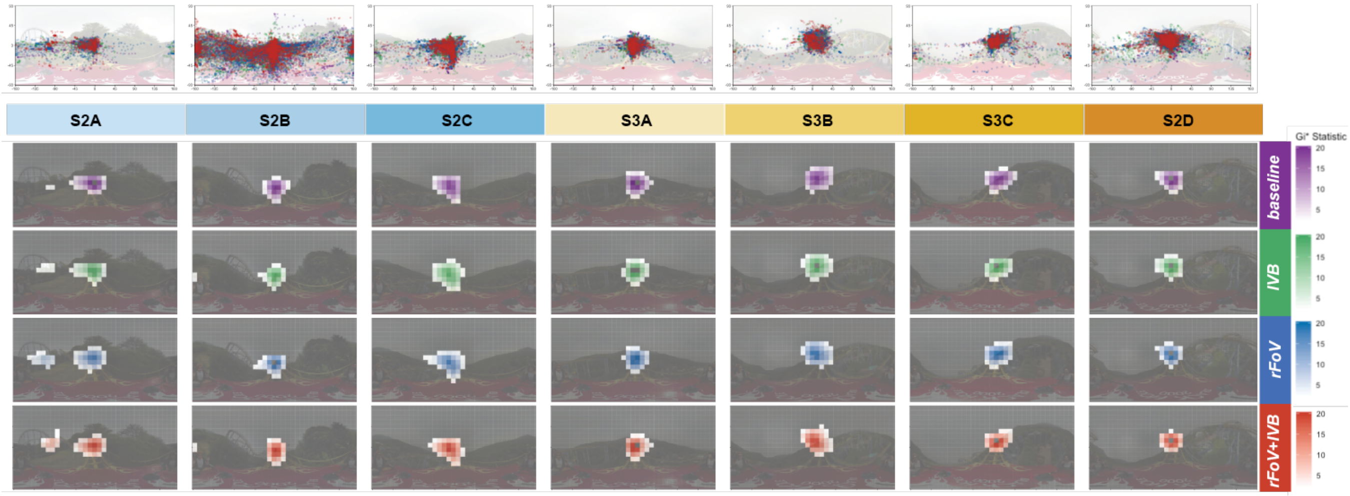

Figure 7: Time series of hotspots for subsections of S2 and S3, considering the full population: x-axis represents time, y-axis from top to bottom: point cloud of head directions, hotspots for baseline, IVB, rFoVand rFoV+IVB

to prevent this by smooth dampening values over 0.3 seconds to prevent extreme flickering, but the values could be adjusted for future iterations.

While the participant behaviour for full population shows that users were focused on the track regardless of condition, a more in-depth analysis of the subpopulations, and supported by statistical significance, shows that the techniques affected behaviour. In the presence of a restricted FoV, the female subpopulation has statistically significant higher distance values for roller coaster segments S2 and S3 (meaning, they explored more) and higher distance to POI values for S3 (meaning, that they focused less on the track during the turbulent portion of the ride). Furthermore, considering the upper 75th subpopulation, a main interaction effect was found for distance (S3-D), meaning that adding an IVB to the restricted FoV resulted in less movement. This suggests that participants experiencing a combination of IVB and restricted FoV were reticent in moving away from the track, positing that a sensory conflict might have emerged and affected the SSQ scores for rFoV+IVB.

7.2 RQ2 - How can we apply/combine techniques that mitigate VIMS in VR to 360° video?

Although our results have limited significance, our data seems to support that the combination of techniques does not bring benefits in terms of mitigating VIMS; in fact, the complexity of the techniques (e.g., dynamic restriction from the optical flow) and the visual incongruence between optimizations, seems to suggest that the techniques were too distracting (reducing Presence scores) and did not adequately mitigate VIMS (increasing SSQ scores). The application of VIMS techniques such as IVB and restricted FoV using optical flow is successful but needs further work. Using only a restricted FoV (rFoV), not only presented the lowest SSQ mean scores but was well received in terms of comfort, enjoyability, and desire. For this reason, this technique would be the preferred method for future creators/researchers.

7.3 Implications for Design & Future Work

Combining results from both RQs, we posit suggestions for the use of optical flow to mitigate VIMS. While optical flow can identify portions of the video able of inducing VIMS and be successfully applied to VIMS reduction techniques, the characteristics of the video itself (e.g., the existence of a POI) and the behaviour of users when watching bring another dimension to the equation. A future avenue to explore is the merging of optical flow with data about POIs, either established by the creator as is done by Bala et al. [6], by previous users experience as done by Cook et al. [15] or object identification as done by Huang et al. [31]. Furthermore, and considering the positive results of rFoV, future work can explore optimizations of this technique such as different opacities in the restricted FoV, allowing for the video in the periphery of the FoV to be partially visible as well as reducing the optical flow in that part.

Regarding the limitations of our study, our results are usable for other researchers even though they do not yet show statistical significance for VIMS reduction. Therefore, future work should focus on a study comparing only baseline and rFoV, with a range of 360° (preferably, without a fixed path of movement as the track was for the roller coaster, and with considerable motion) and longer exposure times (as suggested by [64]).

8 CONCLUSION

In this paper, we presented a novel method of using optical flow as a control for VIMS reduction techniques, applied to 360°. We conducted a two-way repeated-measures study with 24 participants using independent visual background and restricted FoV, both controlled by precomputed optical flow. By collecting and analyzing user experience metrics, as well as quantitative data from SSQ and

IPQ, and linking it to the original optical flow,we were able to evaluate the techniques used and our results indicate that these work but further studies/iterations are needed for generalization.

ACKNOWLEDGMENTS

This work has been supported by MITIExcell (M1420-01-0145-FEDER-000002), LARSyS-FCT Plurianual funding 2020-2023 and FCT Ph.D. Grant PD/BD/128330/2017.

REFERENCES

[1] 2015. [Extreme] 360° RollerCoaster at Seoul Grand Park. https://www.youtube.com/watch?v=8lsB-P8nGSM

[2] 2017. Introduction to Best Practices. https://developer.oculus.com/design/latest/concepts/bp_intro/

[3] 2017. Tunneling Demo | Google VR. https://developers.google.com/vr/elements/tunneling

[4] Majed Al Zayer, Isayas B. Adhanom, Paul MacNeilage, and Eelke Folmer. 2019. The Effect of Field-of-View Restriction on Sex Bias in VR Sickness and Spatial Navigation Performance. In *Proceedings of the 2019 CHI Conference on Human Factors in Computing Systems (CHI '19)*. ACM, New York, NY, USA, 354:1–354:12. https://doi.org/10.1145/3290605.3300584

[5] Simon Baker and Iain Matthews. 2004. Lucas-Kanade 20 Years On: A Unifying Framework. *International Journal of Computer Vision* 56, 3 (Feb. 2004), 221–255. https://doi.org/10.1023/B:VISI.0000011205.11775.fd

[6] Paulo Bala, Raul Masu, Valentina Nisi, and Nuno Nunes. 2019. "When the Elephant Trumps": A Comparative Study on Spatial Audio for Orientation in 360° Videos. In *Proceedings of the 2019 CHI Conference on Human Factors in Computing Systems (CHI '19)*. ACM, New York, NY, USA, 695:1–695:13. https://doi.org/10.1145/3290605.3300925

[7] A. Berthoz, B. Pavard, and L. R. Young. 1975. Perception of linear horizontal self-motion induced by peripheral vision (linearvection) basic characteristics and visual-vestibular interactions. *Experimental Brain Research* 23, 5 (Nov. 1975), 471–489.

[8] Jiwan Bhandari, Paul MacNeilage, and Eelke Folmer. 2018. Teleportation without spatial disorientation using optical flow cues. In *Proceedings of Graphics Interface*, Vol. 2018.

[9] Roger Bivand, L. Anselin, O. Berke, A. Bernat, M. Carvalho, Y. Chun, C. F. Dormann, S. Dray, R. Halbersma, and N. Lewin-Koh. 2011. *spdep: Spatial dependence: weighting schemes, statistics and models*. R package version 0.5-31, URL http://CRAN. R-project. org/package= spdep.

[10] Roger Bivand, Tim Keitt, Barry Rowlingson, and E. Pebesma. 2014. rgdal: Bindings for the geospatial data abstraction library. *R package version 0.8-16* (2014).

[11] Mark Bolas, J. Adam Jones, Ian McDowall, and Evan Suma. 2017. Dynamic field of view throttling as a means of improving user experience in head mounted virtual environments.

[12] Doug A. Bowman, Ernst Kruijff, Joseph J. LaViola, and Ivan Poupyrev. 2004. *3D User Interfaces: Theory and Practice*. Addison Wesley Longman Publishing Co., Inc., Redwood City, CA, USA.

[13] Th. Brandt, Johannes Dichgans, and Ed Koenig. 1973. Differential effects of central versus peripheral vision on egocentric and exocentric motion perception. *Experimental Brain Research* 16, 5 (March 1973), 476–491. https://doi.org/10.1007/BF00234474

[14] Mi-Hyun Choi, Soo-Jeong Lee, Hyo-Sung Kim, Jae-Woong Yang, Jin-Seung Choi, Gye-Rae Tack, Bongsoo Lee, Soon-Cheol Chung, Soo-Young Min, and Byung-Chan Min. 2009. Long-term study of simulator sickness: differences in psychophysiological responses due to individual sensitivity. In *2009 International Conference on Mechatronics and Automation*. IEEE, 20–25.

[15] Henry E. Cook, Justin A. Hassebrock, and L. James Smart. 2018. Responding to Other People's Posture: Visually Induced Motion Sickness From Naturally Generated Optic Flow. *Frontiers in Psychology* 9 (2018), 1901. https://doi.org/10.3389/fpsyg.2018.01901

[16] Simon Davis, Keith Nesbitt, and Eugene Nalivaiko. 2015. Comparing the onset of cybersickness using the Oculus Rift and two virtual roller coasters. In *Proceedings of the 11th Australasian Conference on Interactive Entertainment (IE 2015)*, Vol. 27. 30. http://crpit.com/confpapers/CRPITV167Davis.pdf

[17] M. H. Draper, E. S. Viire, T. A. Furness, and V. J. Gawron. 2001. Effects of image scale and system time delay on simulator sickness within head-coupled virtual environments. *Human Factors* 43, 1 (2001), 129–146. https://doi.org/10.1518/001872001775992552

[18] Huiyu Duan, Guangtao Zhai, Xiongkuo Min, Yucheng Zhu, Wei Sun, and Xiaokang Yang. 2017. Assessment of Visually Induced Motion Sickness in Immersive Videos. In *Advances in Multimedia Information Processing —PCM 2017 (Lecture Notes in Computer Science)*. Springer, Cham, 662–672. https://doi.org/10.1007/978-3-319-77380-3_63

[19] Henry Been-Lirn Duh, Donald E. Parker, and Thomas A. Furness. 2001. An "Independent Visual Background" Reduced Balance Disturbance Envoked by Visual Scene Motion: Implication for Alleviating Simulator Sickness *(CHI '01)*. Association for Computing Machinery, New York, NY, USA, 85–89. https://doi.org/10.1145/365024.365051

[20] Henry Been-Lirn Duh, Donald E. Parker, and Thomas A. Furness. 2004. An Independent Visual Background Reduced Simulator Sickness in a Driving Simulator. *Presence: Teleoperators and Virtual Environments* 13, 5 (2004), 578–588. https://doi.org/10.1162/1054746042545283 arXiv:https://doi.org/10.1162/1054746042545283

[21] Natalia Dużmańska, Paweł Strojny, and Agnieszka Strojny. 2018. Can Simulator Sickness Be Avoided? A Review on Temporal Aspects of Simulator Sickness. *Frontiers in Psychology* 9 (Nov. 2018). https://doi.org/10.3389/fpsyg.2018.02132

[22] Sheldon M. Ebenholtz. 2001. *Oculomotor systems and perception*. Cambridge University Press, New York.

[23] Gunnar Farnebäck. 2003. Two-frame motion estimation based on polynomial expansion. *Image analysis* (2003), 363–370.

[24] Ajoy S. Fernandes and Steven K. Feiner. 2016. Combating VR sickness through subtle dynamic field-of-view modification. In *2016 IEEE Symposium on 3D User Interfaces (3DUI)*. 201–210. https://doi.org/10.1109/3DUI.2016.7460053

[25] Jos Feys. 2016. Nonparametric tests for the interaction in two-way factorial designs using R. *The R Journal* 8, 1 (2016), 367–378.

[26] Andy Field, Jeremy Miles, and Zoë Field. 2012. *Discovering statistics using R*. Sage publications.

[27] Moira B. Flanagan, James G. May, and Thomas G. Dobie. 2005. Sex differences in tolerance to visually-induced motion sickness. *Aviation, space, and environmental medicine* 76, 7 (2005), 642–646.

[28] Augusto Garcia-Agundez, Aiko Westmeier, Polona Caserman, Robert Konrad, and Stefan Göbel. 2017. An Evaluation of Extrapolation and Filtering Techniques in Head Tracking for Virtual Environments to Reduce Cybersickness. In *Serious Games (Lecture Notes in Computer Science)*. Springer, Cham, 203–211. https://doi.org/10.1007/978-3-319-70111-0_19

[29] John F Golding. 1998. Motion sickness susceptibility questionnaire revised and its relationship to other forms of sickness. *Brain Research Bulletin* 47, 5 (Nov. 1998), 507–516. https://doi.org/10.1016/S0361-9230(98)00091-4

[30] Peter A. Howarth and Simon G. Hodder. 2008. Characteristics of habituation to motion in a virtual environment. *Displays* 29, 2 (2008), 117 – 123. https://doi.org/10.1016/j.displa.2007.09.009 Health and Safety Aspects of Visual Displays.

[31] Haikun Huang, Michael Solah, Dingzeyu Li, and Lap-Fai Yu. 2019. Audible Panorama: Automatic Spatial Audio Generation for Panorama Imagery. In *Proceedings of the 2019 CHI Conference on Human Factors in Computing Systems (CHI '19)*. ACM, New York, NY, USA, 621:1–621:11. https://doi.org/10.1145/3290605.3300851

[32] J. Adam Jones, David M. Krum, and Mark T. Bolas. 2017. Vertical field-of-view extension and walking characteristics in head-worn virtual environments. *ACM Transactions on Applied Perception (TAP)* 14, 2 (2017), 9.

[33] Nupur Kala, Kyungmin Lim, Kwanghyun Won, Jaesung Lee, Tammy Lee, Sehoon Kim, and Wonhee Choe. 2017. P-218: An Approach to Reduce VR Sickness by Content Based Field of View Processing. *SID Symposium Digest of Technical Papers* 48, 1 (May 2017), 1645–1648. https://doi.org/10.1002/sdtp.11956

[34] Shunichi Kasahara, Shohei Nagai, and Jun Rekimoto. 2015. First Person Omnidirectional Video: System Design and Implications for Immersive Experience *(TVX '15)*. Association for Computing Machinery, New York, NY, USA, 33–42. https://doi.org/10.1145/2745197.2745202

[35] Robert S. Kennedy, Norman E. Lane, Kevin S. Berbaum, and Michael G. Lilienthal. 1993. Simulator Sickness Questionnaire: An Enhanced Method for Quantifying Simulator Sickness. *The International Journal of Aviation Psychology* 3, 3 (July 1993), 203–220. https://doi.org/10.1207/s15327108ijap0303_3

[36] Behrang Keshavarz, Heiko Hecht, and Lisa Zschutschke. 2011. Intra-visual conflict in visually induced motion sickness. *Displays* 32, 4 (Oct. 2011), 181–188. https://doi.org/10.1016/j.displa.2011.05.009

[37] Nam-Gyoon Kim and Beom-Su Kim. 2019. The Effect of Retinal Eccentricity on Visually Induced Motion Sickness and Postural Control. *Applied Sciences* 9 (05 2019), 1–9. https://doi.org/10.3390/app9091919

[38] Young Youn Kim, Eun Nam Kim, Min Jae Park, Kwang Suk Park, Hee Dong Ko, and Hyun Taek Kim. 2008. The Application of Biosignal Feedback for Reducing Cybersickness from Exposure to a Virtual Environment. *Presence* 17, 1 (Feb. 2008), 1–16. https://doi.org/10.1162/pres.17.1.1

[39] Joseph J. LaViola, Jr. 2000. A Discussion of Cybersickness in Virtual Environments. *SIGCHI Bull.* 32, 1 (Jan. 2000), 47–56. https://doi.org/10.1145/333329.333344

[40] Jiun-Yu Lee, Ping-Hsuan Han, Ling Tsai, Rih-Ding Peng, Yang-Sheng Chen, Kuan-Wen Chen, and Yi-Ping Hung. 2017. Estimating the Simulator Sickness in Immersive Virtual Reality with Optical Flow Analysis. In *SIGGRAPH Asia 2017 Posters (SA '17)*. ACM, New York, NY, USA, 16:1–16:2. https://doi.org/10.1145/3145690.3145697

[41] James Jeng-Weei Lin, Habib Abi-Rached, Do-Hoe Kim, Donald E. Parker, and Thomas A. Furness. 2002. A "Natural" Independent Visual Background Reduced Simulator Sickness. *Proceedings of the Human Factors and Ergonomics*

Society Annual Meeting 46, 26 (2002), 2124–2128. https://doi.org/10.1177/154193120204602605 arXiv:https://doi.org/10.1177/154193120204602605

[42] Wen-Chih Lo, Ching-Ling Fan, Jean Lee, Chun-Ying Huang, Kuan-Ta Chen, and Cheng-Hsin Hsu. 2017. 360° Video Viewing Dataset in Head-Mounted Virtual Reality. In *Proceedings of the 8th ACM on Multimedia Systems Conference (MMSys'17)*. ACM, New York, NY, USA, 211–216. https://doi.org/10.1145/3083187.3083219

[43] Ville Mäkelä, Tuuli Keskinen, John Mäkelä, Pekka Kallioniemi, Jussi Karhu, Kimmo Ronkainen, Alisa Burova, Jaakko Hakulinen, and Markku Turunen. 2019. What Are Others Looking at? Exploring 360° Videos on HMDs with Visual Cues about Other Viewers *(TVX '19)*. Association for Computing Machinery, New York, NY, USA, 13–24. https://doi.org/10.1145/3317697.3323351

[44] Mark McGill, Alexander Ng, and Stephen Brewster. 2017. I Am The Passenger: How Visual Motion Cues Can Influence Sickness For In-Car VR. In *Proceedings of the 2017 CHI Conference on Human Factors in Computing Systems (CHI '17)*. ACM, New York, NY, USA, 5655–5668. https://doi.org/10.1145/3025453.3026046

[45] Doug McIlroy, Ray Brownrigg, Thomas P. Minka, and Roger Bivand. 2014. Mapproj: map projections. *R package version* (2014), 1–2.

[46] Jason D. Moss and Eric R. Muth. 2011. Characteristics of Head-Mounted Displays and Their Effects on Simulator Sickness. *Human Factors: The Journal of the Human Factors and Ergonomics Society* 53, 3 (June 2011), 308–319. https://doi.org/10.1177/0018720811405196

[47] Justin Munafo, Meg Diedrick, and Thomas A. Stoffregen. 2017. The virtual reality head-mounted display Oculus Rift induces motion sickness and is sexist in its effects. *Experimental brain research* 235, 3 (2017), 889–901.

[48] Mahdi Nabiyouni and Doug A. Bowman. 2016. A Taxonomy for Designing Walking-based Locomotion Techniques for Virtual Reality. In *Proceedings of the 2016 ACM Companion on Interactive Surfaces and Spaces (ISS Companion '16)*. ACM, New York, NY, USA, 115–121. https://doi.org/10.1145/3009939.3010076

[49] Anh Nguyen and Zhisheng Yan. 2019. A Saliency Dataset for 360-degree Videos. In *Proceedings of the 10th ACM Multimedia Systems Conference (MMSys '19)*. ACM, New York, NY, USA, 279–284. https://doi.org/10.1145/3304109.3325820

[50] Cuong Nguyen, Stephen DiVerdi, Aaron Hertzmann, and Feng Liu. 2017. Vremiere: In-Headset Virtual Reality Video Editing. In *Proceedings of the 2017 CHI Conference on Human Factors in Computing Systems (CHI '17)*. ACM, New York, NY, USA, 5428–5438. https://doi.org/10.1145/3025453.3025675

[51] George D. Park, R. Wade Allen, Dary Fiorentino, Theodore J. Rosenthal, and Marcia L. Cook. 2006. Simulator sickness scores according to symptom susceptibility, age, and gender for an older driver assessment study. In *Proceedings of the human factors and ergonomics society annual meeting*, Vol. 50. SAGE Publications Sage CA: Los Angeles, CA, 2702–2706.

[52] Edzer Pebesma. 2018. Simple Features for R: Standardized Support for Spatial Vector Data. *The R Journal* 10, 1 (2018), 439–446. https://doi.org/10.32614/RJ-2018-009

[53] J. D. Prothero, M. H. Draper, T. A. Furness, D. E. Parker, and M. J. Wells. 1999. The use of an independent visual background to reduce simulator side-effects. *Aviation, Space, and Environmental Medicine* 70, 3 Pt 1 (March 1999), 277–283.

[54] R Core Team. 2014. *R: A Language and Environment for Statistical Computing*. R Foundation for Statistical Computing, Vienna, Austria. http://www.R-project.org/

[55] Sharif Razzaque, Zachariah Kohn, and Mary C Whitton. 2001. *Redirected Walking*. Technical Report. University of North Carolina at Chapel Hill, Chapel Hill, NC, USA.

[56] Lisa Rebenitsch and Charles Owen. 2014. Individual Variation in Susceptibility to Cybersickness. In *Proceedings of the 27th Annual ACM Symposium on User Interface Software and Technology (UIST '14)*. ACM, New York, NY, USA, 309–317. https://doi.org/10.1145/2642918.2647394

[57] Lisa Rebenitsch and Charles Owen. 2016. Review on cybersickness in applications and visual displays. *Virtual Reality* 20, 2 (June 2016), 101–125. https://doi.org/10.1007/s10055-016-0285-9

[58] Gary E. Riccio and Thomas A. Stoffregen. 1991. An ecological Theory of Motion Sickness and Postural Instability. *Ecological Psychology* 3, 3 (Sept. 1991), 195–240. https://doi.org/10.1207/s15326969eco0303_2

[59] Sylvia Rothe and Heinrich Hußmann. 2018. Spatial statistics for analyzing data in cinematic virtual reality. In *Proceedings of the 2018 International Conference on Advanced Visual Interfaces - AVI '18*. ACM Press, Castiglione della Pescaia, Grosseto, Italy, 1–3. https://doi.org/10.1145/3206505.3206561

[60] Santeri Saarinen, Ville Mäkelä, Pekka Kallioniemi, Jaakko Hakulinen, and Markku Turunen. 2017. Guidelines for Designing Interactive Omnidirectional Video Applications. In *16th IFIP TC 13 International Conference on Human-Computer Interaction — INTERACT 2017 - Volume 10516*. Springer-Verlag, Berlin, Heidelberg, 263–272. https://doi.org/10.1007/978-3-319-68059-0_17

[61] Timothy Scaffidi. 2018. ofxOpticalFlowFarneback: openFrameworks addon for gunnar-farneback dense optical flow method. https://github.com/timscaffidi/ofxOpticalFlowFarneback original-date: 2012-11-13T08:43:28Z.

[62] Thomas Schubert, Frank Friedmann, and Holger Regenbrecht. 2001. The Experience of Presence: Factor Analytic Insights. *Presence: Teleoper. Virtual Environ.* 10, 3 (June 2001), 266–281. https://doi.org/10.1162/105474601300343603

[63] Mel Slater and Maria V. Sanchez-Vives. 2016. Enhancing Our Lives with Immersive Virtual Reality. *Frontiers in Robotics and AI* 3 (Dec. 2016). https://doi.org/10.3389/frobt.2016.00074

[64] Kay M. Stanney, D. Susan Lanham, Robert S. Kennedy, and Robert Breaux. 1999. Virtual Environment Exposure Drop-Out Thresholds. *Proceedings of the Human Factors and Ergonomics Society Annual Meeting* 43, 22 (1999), 1223–1227. https://doi.org/10.1177/154193129904302212

[65] Sam Tregillus. 2016. VR-Drop: Exploring the Use of Walking-in-Place to Create Immersive VR Games. In *Proceedings of the 2016 CHI Conference Extended Abstracts on Human Factors in Computing Systems (CHI EA '16)*. ACM, New York, NY, USA, 176–179. https://doi.org/10.1145/2851581.2890374

[66] M. Treisman. 1977. Motion sickness: an evolutionary hypothesis. *Science (New York, N.Y.)* 197, 4302 (July 1977), 493–495. https://doi.org/10.1126/science.301659

[67] Michael Venturino and Maxwell J. Wells. 1990. Head Movements as a Function of Field-of-View Size on a Helmet-Mounted Display. *Proceedings of the Human Factors Society Annual Meeting* 34, 19 (Oct. 1990), 1572–1576. https://doi.org/10.1177/154193129003401932

[68] David Matthew Whittinghill, Bradley Ziegler, T Case, and B Moore. 2015. Nasum virtualis: A simple technique for reducing simulator sickness. In *Games Developers Conference (GDC)*. 74.

[69] Hadley Wickham. 2009. *ggplot2: Elegant Graphics for Data Analysis*. Springer-Verlag New York. http://ggplot2.org

[70] Bob G. Witmer and Michael J. Singer. 1998. Measuring Presence in Virtual Environments: A Presence Questionnaire. *Presence: Teleoperators and Virtual Environments* 7, 3 (June 1998), 225–240. https://doi.org/10.1162/105474698565686

[71] Jacob O. Wobbrock, Leah Findlater, Darren Gergle, and James J. Higgins. 2011. The Aligned Rank Transform for Nonparametric Factorial Analyses Using Only Anova Procedures. In *Proceedings of the SIGCHI Conference on Human Factors in Computing Systems (CHI '11)*. ACM, New York, NY, USA, 143–146. https://doi.org/10.1145/1978942.1978963

[72] Robert Xiao and Hrvoje Benko. 2016. Augmenting the Field-of-View of Head-Mounted Displays with Sparse Peripheral Displays. In *Proceedings of the 2016 CHI Conference on Human Factors in Computing Systems (CHI '16)*. ACM, New York, NY, USA, 1221–1232. https://doi.org/10.1145/2858036.2858212